

**Identified hadron spectra at large transverse  
momentum in  $p+p$  and  $d+Au$  collisions at  
 $\sqrt{s_{NN}} = 200 \text{ GeV}$**

J. Adams<sup>b</sup>, M.M. Aggarwal<sup>ac</sup>, Z. Ahammed<sup>ar</sup>, J. Amonett<sup>s</sup>,  
 B.D. Anderson<sup>s</sup>, M. Anderson<sup>f</sup>, D. Arkhipkin<sup>l</sup>,  
 G.S. Averichev<sup>k</sup>, S.K. Badyal<sup>r</sup>, Y. Bai<sup>aa</sup>, J. Balewski<sup>p</sup>,  
 O. Barannikova<sup>af</sup>, L.S. Barnby<sup>b</sup>, J. Baudot<sup>q</sup>, S. Bekele<sup>ab</sup>,  
 V.V. Belaga<sup>k</sup>, A. Bellingeri-Laurikainen<sup>am</sup>, R. Bellwied<sup>au</sup>,  
 B.I. Bezverkhny<sup>aw</sup>, S. Bharadwaj<sup>ah</sup>, A. Bhasin<sup>r</sup>, A.K. Bhati<sup>ac</sup>,  
 H. Bichsel<sup>at</sup>, J. Bielcik<sup>aw</sup>, J. Bielcikova<sup>aw</sup>, A. Billmeier<sup>au</sup>,  
 L.C. Bland<sup>c</sup>, C.O. Blyth<sup>b</sup>, S-L. Blyth<sup>u</sup>, B.E. Bonner<sup>ai</sup>,  
 M. Botje<sup>aa</sup>, J. Bouchet<sup>am</sup>, A.V. Brandin<sup>y</sup>, A. Bravar<sup>c</sup>,  
 M. Bystersky<sup>j</sup>, R.V. Cadman<sup>a</sup>, X.Z. Cai<sup>al</sup>, H. Caines<sup>aw</sup>,  
 M. Calderón de la Barca Sánchez<sup>f</sup>, J. Castillo<sup>aa</sup>, O. Catu<sup>aw</sup>,  
 D. Cebra<sup>f</sup>, Z. Chajecki<sup>ab</sup>, P. Chaloupka<sup>j</sup>, S. Chattopadhyay<sup>ar</sup>,  
 H.F. Chen<sup>ak</sup>, J.H. Chen<sup>al</sup>, Y. Chen<sup>g</sup>, J. Cheng<sup>ap</sup>, M. Cherney<sup>i</sup>,  
 A. Chikanian<sup>aw</sup>, H.A. Choi<sup>ag</sup>, W. Christie<sup>c</sup>, J.P. Coffin<sup>q</sup>,  
 T.M. Cormier<sup>au</sup>, M.R. Cosentino<sup>aj</sup>, J.G. Cramer<sup>at</sup>,  
 H.J. Crawford<sup>e</sup>, D. Das<sup>ar</sup>, S. Das<sup>ar</sup>, M. Daugherty<sup>ao</sup>,  
 M.M. de Moura<sup>aj</sup>, T.G. Dedovich<sup>k</sup>, M. DePhillips<sup>c</sup>,  
 A.A. Derevschikov<sup>ae</sup>, L. Didenko<sup>c</sup>, T. Dietel<sup>m</sup>, P. Djawotho<sup>p</sup>,  
 S.M. Dogra<sup>r</sup>, W.J. Dong<sup>g</sup>, X. Dong<sup>ak</sup>, J.E. Draper<sup>f</sup>, F. Du<sup>aw</sup>,  
 V.B. Dunin<sup>k</sup>, J.C. Dunlop<sup>c</sup>, M.R. Dutta Mazumdar<sup>ar</sup>,  
 V. Eckardt<sup>w</sup>, W.R. Edwards<sup>u</sup>, L.G. Efimov<sup>k</sup>, V. Emelianov<sup>y</sup>,  
 J. Engelage<sup>e</sup>, G. Eppley<sup>ai</sup>, B. Erazmus<sup>am</sup>, M. Estienne<sup>q</sup>,  
 P. Fachini<sup>c</sup>, R. Fatemi<sup>v</sup>, J. Fedorisin<sup>k</sup>, K. Filimonov<sup>u</sup>,  
 P. Filip<sup>j</sup>, E. Finch<sup>aw</sup>, V. Fine<sup>c</sup>, Y. Fisyak<sup>c</sup>, K.S.F. Fornazier<sup>aj</sup>,  
 J. Fu<sup>av</sup>, C.A. Gagliardi<sup>an</sup>, L. Gaillard<sup>b</sup>, J. Gans<sup>aw</sup>,  
 M.S. Ganti<sup>ar</sup>, V. Ghazikhanian<sup>g</sup>, P. Ghosh<sup>ar</sup>, J.E. Gonzalez<sup>g</sup>,  
 Y.G. Gorbunov<sup>i</sup>, H. Gos<sup>as</sup>, O. Grachov<sup>au</sup>, O. Grebenyuk<sup>aa</sup>,  
 D. Grosnick<sup>aq</sup>, S.M. Guertin<sup>g</sup>, Y. Guo<sup>au</sup>, A. Gupta<sup>r</sup>,  
 N. Gupta<sup>r</sup>, T.D. Gutierrez<sup>f</sup>, B. Haag<sup>f</sup>, T.J. Hallman<sup>c</sup>,

A. Hamed<sup>au</sup>, J.W. Harris<sup>aw</sup>, W. He<sup>p</sup>, M. Heinz<sup>aw</sup>,  
 T.W. Henry<sup>an</sup>, S. Hepplemann<sup>ad</sup>, B. Hippolyte<sup>q</sup>, A. Hirsch<sup>af</sup>,  
 E. Hjort<sup>u</sup>, G.W. Hoffmann<sup>ao</sup>, M.J. Horner<sup>u</sup>, H.Z. Huang<sup>g</sup>,  
 S.L. Huang<sup>ak</sup>, E.W. Hughes<sup>d</sup>, T.J. Humanic<sup>ab</sup>, G. Igo<sup>g</sup>,  
 P. Jacobs<sup>u</sup>, W.W. Jacobs<sup>p</sup>, P. Jakl<sup>j</sup>, F. Jia<sup>t</sup>, H. Jiang<sup>g</sup>,  
 P.G. Jones<sup>b</sup>, E.G. Judd<sup>e</sup>, S. Kabana<sup>am</sup>, K. Kang<sup>ap</sup>,  
 J. Kapitan<sup>j</sup>, M. Kaplan<sup>h</sup>, D. Keane<sup>s</sup>, A. Kechechyan<sup>k</sup>,  
 V.Yu. Khodyrev<sup>ae</sup>, B.C. Kim<sup>ag</sup>, J. Kiryluk<sup>v</sup>, A. Kisiel<sup>as</sup>,  
 E.M. Kislov<sup>k</sup>, S.R. Klein<sup>u</sup>, D.D. Koetke<sup>aq</sup>, T. Kollegger<sup>m</sup>,  
 M. Kopytine<sup>s</sup>, L. Kotchenda<sup>y</sup>, V. Kouchpil<sup>j</sup>, K.L. Kowalik<sup>u</sup>,  
 M. Kramer<sup>z</sup>, P. Kravtsov<sup>y</sup>, V.I. Kravtsov<sup>ae</sup>, K. Krueger<sup>a</sup>,  
 C. Kuhn<sup>q</sup>, A.I. Kulikov<sup>k</sup>, A. Kumar<sup>ac</sup>, A.A. Kuznetsov<sup>k</sup>,  
 M.A.C. Lamont<sup>aw</sup>, J.M. Landgraf<sup>c</sup>, S. Lange<sup>m</sup>, F. Laue<sup>c</sup>,  
 J. Lauret<sup>c</sup>, A. Lebedev<sup>c</sup>, R. Lednicky<sup>k</sup>, C-H. Lee<sup>ag</sup>,  
 S. Lehocka<sup>k</sup>, M.J. LeVine<sup>c</sup>, C. Li<sup>ak</sup>, Q. Li<sup>au</sup>, Y. Li<sup>ap</sup>, G. Lin<sup>aw</sup>,  
 S.J. Lindenbaum<sup>z</sup>, M.A. Lisa<sup>ab</sup>, F. Liu<sup>av</sup>, H. Liu<sup>ak</sup>, J. Liu<sup>ai</sup>,  
 L. Liu<sup>av</sup>, Z. Liu<sup>av</sup>, T. Ljubicic<sup>c</sup>, W.J. Llope<sup>ai</sup>, H. Long<sup>g</sup>,  
 R.S. Longacre<sup>c</sup>, M. Lopez-Noriega<sup>ab</sup>, W.A. Love<sup>c</sup>, Y. Lu<sup>av</sup>,  
 T. Ludlam<sup>c</sup>, D. Lynn<sup>c</sup>, G.L. Ma<sup>al</sup>, J.G. Ma<sup>g</sup>, Y.G. Ma<sup>al</sup>,  
 D. Magestro<sup>ab</sup>, S. Mahajan<sup>r</sup>, D.P. Mahapatra<sup>n</sup>, R. Majka<sup>aw</sup>,  
 L.K. Mangotra<sup>r</sup>, R. Manweiler<sup>aq</sup>, S. Margetis<sup>s</sup>, C. Markert<sup>s</sup>,  
 L. Martin<sup>am</sup>, H.S. Matis<sup>u</sup>, Yu.A. Matulenko<sup>ae</sup>, C.J. McClain<sup>a</sup>,  
 T.S. McShane<sup>i</sup>, Yu. Melnick<sup>ae</sup>, A. Meschanin<sup>ae</sup>, M.L. Miller<sup>v</sup>,  
 M. Milos<sup>j</sup>, N.G. Minaev<sup>ae</sup>, S. Mioduszewski<sup>an</sup>, C. Mironov<sup>s</sup>,  
 A. Mischke<sup>aa</sup>, D.K. Mishra<sup>n</sup>, J. Mitchell<sup>ai</sup>, B. Mohanty<sup>ar</sup>,  
 L. Molnar<sup>af</sup>, C.F. Moore<sup>ao</sup>, D.A. Morozov<sup>ae</sup>, M.G. Munhoz<sup>aj</sup>,  
 B.K. Nandi<sup>o</sup>, S.K. Nayak<sup>r</sup>, T.K. Nayak<sup>ar</sup>, J.M. Nelson<sup>b</sup>,  
 P.K. Netrakanti<sup>ar</sup>, V.A. Nikitin<sup>l</sup>, L.V. Nogach<sup>ae</sup>,  
 S.B. Nurushev<sup>ae</sup>, G. Odyniec<sup>u</sup>, A. Ogawa<sup>c</sup>, V. Okorokov<sup>y</sup>,  
 M. Oldenburg<sup>u</sup>, D. Olson<sup>u</sup>, S.K. Pal<sup>ar</sup>, Y. Panebratsev<sup>k</sup>,  
 S.Y. Panitkin<sup>c</sup>, A.I. Pavlinov<sup>au</sup>, T. Pawlak<sup>as</sup>, T. Peitzmann<sup>aa</sup>,  
 V. Perevoztchikov<sup>c</sup>, C. Perkins<sup>e</sup>, W. Peryt<sup>as</sup>, V.A. Petrov<sup>au</sup>,  
 S.C. Phatak<sup>n</sup>, R. Picha<sup>f</sup>, M. Planinic<sup>ay</sup>, J. Pluta<sup>as</sup>,  
 N. Poljak<sup>ay</sup>, N. Porile<sup>af</sup>, J. Porter<sup>at</sup>, A.M. Poskanzer<sup>u</sup>,  
 M. Potekhin<sup>c</sup>, E. Potrebenikova<sup>k</sup>, B.V.K.S. Potukuchi<sup>r</sup>,

D. Prindle<sup>at</sup>, C. Pruneau<sup>au</sup>, J. Putschke<sup>u</sup>, G. Rakness<sup>ad</sup>,  
 R. Raniwala<sup>ah</sup>, S. Raniwala<sup>ah</sup>, R.L. Ray<sup>ao</sup>, S.V. Razin<sup>k</sup>,  
 J. Reinnarth<sup>am</sup>, D. Relyea<sup>d</sup>, F. Retiere<sup>u</sup>, A. Ridiger<sup>y</sup>,  
 H.G. Ritter<sup>u</sup>, J.B. Roberts<sup>ai</sup>, O.V. Rogachevskiy<sup>k</sup>,  
 J.L. Romero<sup>f</sup>, A. Rose<sup>u</sup>, C. Roy<sup>am</sup>, L. Ruan<sup>u</sup>,  
 M.J. Russcher<sup>aa</sup>, R. Sahoo<sup>n</sup>, I. Sakrejda<sup>u</sup>, S. Salur<sup>aw</sup>,  
 J. Sandweiss<sup>aw</sup>, M. Sarsour<sup>an</sup>, I. Savin<sup>l</sup>, P.S. Sazhin<sup>k</sup>,  
 J. Schambach<sup>ao</sup>, R.P. Scharenberg<sup>af</sup>, N. Schmitz<sup>w</sup>,  
 K. Schweda<sup>u</sup>, J. Seger<sup>i</sup>, I. Selyuzhenkov<sup>au</sup>, P. Seyboth<sup>w</sup>,  
 A. Shabetai<sup>u</sup>, E. Shahaliev<sup>k</sup>, M. Shao<sup>ak</sup>, M. Sharma<sup>ac</sup>,  
 W.Q. Shen<sup>al</sup>, S.S. Shimanskiy<sup>k</sup>, E. Sichtermann<sup>u</sup>, F. Simon<sup>v</sup>,  
 R.N. Singaraju<sup>ar</sup>, N. Smirnov<sup>aw</sup>, R. Snellings<sup>aa</sup>, G. Sood<sup>aq</sup>,  
 P. Sorensen<sup>c</sup>, J. Sowinski<sup>p</sup>, J. Speltz<sup>q</sup>, H.M. Spinka<sup>a</sup>,  
 B. Srivastava<sup>af</sup>, A. Stadnik<sup>k</sup>, T.D.S. Stanislaus<sup>aq</sup>, R. Stock<sup>m</sup>,  
 A. Stolpovsky<sup>au</sup>, M. Strikhanov<sup>y</sup>, B. Stringfellow<sup>af</sup>,  
 A.A.P. Suaide<sup>aj</sup>, E. Sugarbaker<sup>ab</sup>, M. Sumbera<sup>j</sup>, Z. Sun<sup>t</sup>,  
 B. Sorrow<sup>v</sup>, M. Swanger<sup>i</sup>, T.J.M. Symons<sup>u</sup>,  
 A. Szanto de Toledo<sup>aj</sup>, A. Tai<sup>g</sup>, J. Takahashi<sup>aj</sup>, A.H. Tang<sup>c</sup>,  
 T. Tarnowsky<sup>af</sup>, D. Thein<sup>g</sup>, J.H. Thomas<sup>u</sup>, A.R. Timmins<sup>b</sup>,  
 S. Timoshenko<sup>y</sup>, M. Tokarev<sup>k</sup>, T.A. Trainor<sup>at</sup>, S. Trentalange<sup>g</sup>,  
 R.E. Tribble<sup>an</sup>, O.D. Tsai<sup>g</sup>, J. Ulery<sup>af</sup>, T. Ullrich<sup>c</sup>,  
 D.G. Underwood<sup>a</sup>, G. Van Buren<sup>c</sup>, N. van der Kolk<sup>aa</sup>,  
 M. van Leeuwen<sup>u</sup>, A.M. Vander Molen<sup>x</sup>, R. Varma<sup>o</sup>,  
 I.M. Vasilevski<sup>l</sup>, A.N. Vasiliev<sup>ae</sup>, R. Vernet<sup>q</sup>, S.E. Vigdor<sup>p</sup>,  
 Y.P. Viyogi<sup>ar</sup>, S. Vokal<sup>k</sup>, S.A. Voloshin<sup>au</sup>, W.T. Waggoner<sup>i</sup>,  
 F. Wang<sup>af</sup>, G. Wang<sup>s</sup>, J.S. Wang<sup>t</sup>, X.L. Wang<sup>ak</sup>, Y. Wang<sup>ap</sup>,  
 J.W. Watson<sup>s</sup>, J.C. Webb<sup>p</sup>, G.D. Westfall<sup>x</sup>, A. Wetzler<sup>u</sup>,  
 C. Whitten Jr.<sup>g</sup>, H. Wieman<sup>u</sup>, S.W. Wissink<sup>p</sup>, R. Witt<sup>aw</sup>,  
 J. Wood<sup>g</sup>, J. Wu<sup>ak</sup>, N. Xu<sup>u</sup>, Q.H. Xu<sup>u</sup>, Z. Xu<sup>c</sup>, P. Yepes<sup>ai</sup>,  
 I-K. Yoo<sup>ag</sup>, V.I. Yurevich<sup>k</sup>, I. Zborovsky<sup>j</sup>, W. Zhan<sup>t</sup>,  
 H. Zhang<sup>c</sup>, W.M. Zhang<sup>s</sup>, Y. Zhang<sup>ak</sup>, Z.P. Zhang<sup>ak</sup>,  
 Y. Zhao<sup>ak</sup>, C. Zhong<sup>al</sup>, R. Zoukarneev<sup>l</sup>, Y. Zoukarneeva<sup>l</sup>,  
 A.N. Zubarev<sup>k</sup> and J.X. Zuo<sup>al</sup>

(STAR Collaboration)

<sup>a</sup>Argonne National Laboratory, Argonne, Illinois 60439

- <sup>b</sup> *University of Birmingham, Birmingham, United Kingdom*
- <sup>c</sup> *Brookhaven National Laboratory, Upton, New York 11973*
- <sup>d</sup> *California Institute of Technology, Pasadena, California 91125*
- <sup>e</sup> *University of California, Berkeley, California 94720*
- <sup>f</sup> *University of California, Davis, California 95616*
- <sup>g</sup> *University of California, Los Angeles, California 90095*
- <sup>h</sup> *Carnegie Mellon University, Pittsburgh, Pennsylvania 15213*
- <sup>i</sup> *Creighton University, Omaha, Nebraska 68178*
- <sup>j</sup> *Nuclear Physics Institute AS CR, 250 68 Řež/Prague, Czech Republic*
- <sup>k</sup> *Laboratory for High Energy (JINR), Dubna, Russia*
- <sup>l</sup> *Particle Physics Laboratory (JINR), Dubna, Russia*
- <sup>m</sup> *University of Frankfurt, Frankfurt, Germany*
- <sup>n</sup> *Institute of Physics, Bhubaneswar 751005, India*
- <sup>o</sup> *Indian Institute of Technology, Mumbai, India*
- <sup>p</sup> *Indiana University, Bloomington, Indiana 47408*
- <sup>q</sup> *Institut de Recherches Subatomiques, Strasbourg, France*
- <sup>r</sup> *University of Jammu, Jammu 180001, India*
- <sup>s</sup> *Kent State University, Kent, Ohio 44242*
- <sup>t</sup> *Institute of Modern Physics, Lanzhou, P.R. China*
- <sup>u</sup> *Lawrence Berkeley National Laboratory, Berkeley, California 94720*
- <sup>v</sup> *Massachusetts Institute of Technology, Cambridge, MA 02139-4307*
- <sup>w</sup> *Max-Planck-Institut für Physik, Munich, Germany*
- <sup>x</sup> *Michigan State University, East Lansing, Michigan 48824*
- <sup>y</sup> *Moscow Engineering Physics Institute, Moscow Russia*
- <sup>z</sup> *City College of New York, New York City, New York 10031*
- <sup>aa</sup> *NIKHEF and Utrecht University, Amsterdam, The Netherlands*
- <sup>ab</sup> *Ohio State University, Columbus, Ohio 43210*
- <sup>ac</sup> *Panjab University, Chandigarh 160014, India*
- <sup>ad</sup> *Pennsylvania State University, University Park, Pennsylvania 16802*
- <sup>ae</sup> *Institute of High Energy Physics, Protvino, Russia*
- <sup>af</sup> *Purdue University, West Lafayette, Indiana 47907*
- <sup>ag</sup> *Pusan National University, Pusan, Republic of Korea*
- <sup>ah</sup> *University of Rajasthan, Jaipur 302004, India*
- <sup>ai</sup> *Rice University, Houston, Texas 77251*
- <sup>aj</sup> *Universidade de Sao Paulo, Sao Paulo, Brazil*
- <sup>ak</sup> *University of Science & Technology of China, Hefei 230026, China*

<sup>al</sup> *Shanghai Institute of Applied Physics, Shanghai 201800, China*

<sup>am</sup> *SUBATECH, Nantes, France*

<sup>an</sup> *Texas A&M University, College Station, Texas 77843*

<sup>ao</sup> *University of Texas, Austin, Texas 78712*

<sup>ap</sup> *Tsinghua University, Beijing 100084, China*

<sup>aq</sup> *Valparaiso University, Valparaiso, Indiana 46383*

<sup>ar</sup> *Variable Energy Cyclotron Centre, Kolkata 700064, India*

<sup>as</sup> *Warsaw University of Technology, Warsaw, Poland*

<sup>at</sup> *University of Washington, Seattle, Washington 98195*

<sup>au</sup> *Wayne State University, Detroit, Michigan 48201*

<sup>av</sup> *Institute of Particle Physics, CCNU (HZNU), Wuhan 430079, China*

<sup>aw</sup> *Yale University, New Haven, Connecticut 06520*

<sup>ay</sup> *University of Zagreb, Zagreb, HR-10002, Croatia*

---

## Abstract

We present the transverse momentum ( $p_T$ ) spectra for identified charged pions, protons and anti-protons from  $p+p$  and  $d+Au$  collisions at  $\sqrt{s_{NN}} = 200$  GeV. The spectra are measured around midrapidity ( $|y| < 0.5$ ) over the range of  $0.3 < p_T < 10$  GeV/ $c$  with particle identification from the ionization energy loss and its relativistic rise in the Time Projection Chamber and Time-of-Flight in STAR. The charged pion and proton+anti-proton spectra at high  $p_T$  in  $p+p$  and  $d+Au$  collisions are in good agreement with a phenomenological model (EPOS) and with the next-to-leading order perturbative quantum chromodynamic (NLO pQCD) calculations with a specific fragmentation scheme and factorization scale. We found that all proton, anti-proton and charged pion spectra in  $p+p$  collisions follow  $x_T$ -scalings for the momentum range where particle production is dominated by hard processes ( $p_T \gtrsim 2$  GeV/ $c$ ). The nuclear modification factor around midrapidity are found to be greater than unity for charged pions and to be even larger for protons at  $2 < p_T < 5$  GeV/ $c$ .

*Key words:* Particle production, perturbative quantum chromodynamics, fragmentation function, Cronin effect and  $x_T$  scaling.

---

## 1 Introduction

The study of identified hadron spectra at large transverse momentum ( $p_T$ ) in  $p+p$  collisions can be used to test the predictions from perturbative quantum chromodynamics (pQCD) [1]. In the framework of models based on QCD, the

inclusive production of single hadrons is described by the convolution of parton distribution functions (PDF), parton interaction cross-sections and fragmentation functions (FFs). The FFs [2] give the probability for a hard scattered parton to fragment into a hadron of a given momentum fraction. These are not yet calculable from the first principles and hence are generally obtained from experimental data (e.g.,  $e^+e^-$  collisions). The factorization theorem for cross-sections assumes that FFs are independent of the process in which they have been determined and hence represent a universal property of hadronization. It is therefore possible to make quantitative predictions for other types of collision systems (e.g.,  $p+p$ ). Comparisons between experimental data and theory can help to constrain the quark and gluon FFs that are critical to predictions of hadron spectra in  $p+p$ ,  $p+A$ , and  $A+A$  collisions. The simultaneous study of identified hadron  $p_T$  spectra in  $p+p$  and  $d+Au$  collisions may also provide important information on the PDFs [3] of the nucleus. The PDF provides the probability of finding a parton (a quark or a gluon) in a hadron as a function of the fraction of the hadron's momentum carried by the parton.

Within the framework of pQCD, the expected initial-state nuclear effects in  $d+Au$  collisions are multiple scattering (Cronin effect [4]) and shadowing of the parton distribution function. It has been predicted theoretically that, at sufficiently high beam energy, gluon saturation will be the dominant effect, resulting in a state of color glass condensate [5]. A detailed study of particle spectra with respect to rapidity and beam species ( $p+p$ ,  $p+A$ ) is exploitive in understanding the evolution of the parton distribution function.

The study of particle ratios at high  $p_T$  constrains particle production models and also gives unique data on FF ratios, although extraction of this information is model-dependent. For example, the  $p/\pi^+$  ratio reflects the relative probability of a parton to fragment into proton or pion at high  $p_T$  [6]. The high  $p_T$  dependence of  $\bar{p}/p$  ratio in turn reflects the relative contribution of quark and gluon jets to particle production [7].

The identified particle spectra in  $p+p$  and  $d+Au$  collisions also provide reference spectra for the particle production at high  $p_T$  in  $Au+Au$  collisions. Moreover, studies of identified particle production as a function of  $p_T$  in high-energy heavy-ion collisions have revealed many unique features in different  $p_T$  regions [8–11] and between baryons and mesons [12]. A good description of both identified pion and proton spectra in  $p+p$  and  $d+Au$  collisions at the intermediate and high  $p_T$  by NLO pQCD will provide a solid ground for models based on jet quenching [13] and quark recombination [10]. These emphasize the need for a systematic study of the  $p_T$  spectra from  $p+p$  and  $d+Au$  collisions at the same energy as the nucleus-nucleus collisions.

In this letter, we present the  $p_T$  spectra for identified pions, protons and anti-protons in  $p+p$  and  $d+Au$  collisions at  $\sqrt{s_{NN}} = 200$  GeV as measured by

the STAR experiment at RHIC. The results are compared to NLO pQCD calculations and a phenomenological model. We also study the  $x_T$  scaling in  $p+p$  collisions and the Cronin effect in  $d+Au$  collisions.

## 2 Experiment and Analysis

The STAR experiment consists of several detectors to measure hadronic and electromagnetic observables spanning a large region of the available phase space at RHIC. The detectors used in the present analysis are the Time Projection Chamber (TPC), the Time-Of-Flight (TOF) detector, a set of trigger detectors used for obtaining the minimum bias data, and the Forward Time Projection Chamber for the collision centrality determination in  $d+Au$  collisions. The details of the design and other characteristics of the detectors can be found in Ref. [14].

A total of 8.2 million minimum bias  $p+p$  collision events and 11.7 million  $d+Au$  collision events have been analyzed for the present study. The data set has been collected during the years 2001 and 2003. The details of minimum bias trigger conditions for  $p+p$  and  $d+Au$  collisions can be found in the Refs. [15,16]. The minimum-bias trigger captured  $95 \pm 3\%$  of the  $2.21 \pm 0.09$  barn  $d+Au$  inelastic cross-section. The trigger efficiency was determined from a cross study of two sets of trigger detectors: two Zero-Degree Calorimeters (ZDCs) and two beam-beam counters (BBCs). The absolute cross-section is derived from a Monte Carlo Glauber calculation. These results are consistent with other recent measurements [17]. The trigger for the minimum bias  $p+p$  collisions required a coincidence measurement of the two BBCs covering  $3.3 < |\eta| < 5.0$  [18]. This trigger was sensitive to color exchange hadronic and doubly-diffractive events; here, these are labelled "non-singly diffractive (NSD) events". Using PYTHIA(v6.205) [19] and HERWIG [20], it was determined that the trigger measured 87% of the  $30.0 \pm 3.5$  mb NSD cross-section, which was measured via a vernier scan [21].

The data from TOF is used to obtain the identified hadron spectra for  $p_T < 2.5$  GeV/ $c$ . The procedure for particle identification in TOF has been described in Ref. [22]. For  $p_T > 2.5$  GeV/ $c$ , we use data from the TPC. Particle identification at high  $p_T$  in the TPC comes from the relativistic rise of the ionization energy loss ( $rdE/dx$ ). Details of the method are described in Ref. [23]. At  $p_T \gtrsim 3$  GeV/ $c$ , the pion  $dE/dx$  is about 10–20% higher than that of kaons and protons due to the relativistic rise, resulting in a few sigmas ( $1-3\sigma$ ) separation between them. Since pions are the dominant component of the hadrons in  $p+p$  and  $d+Au$  collisions at RHIC, the prominent pion peak in the  $dE/dx$  distribution is fit with a Gaussian to extract the pion yield [23]. The proton yield is obtained by integrating the entries ( $Y$ ) in the low part of the  $dE/dx$

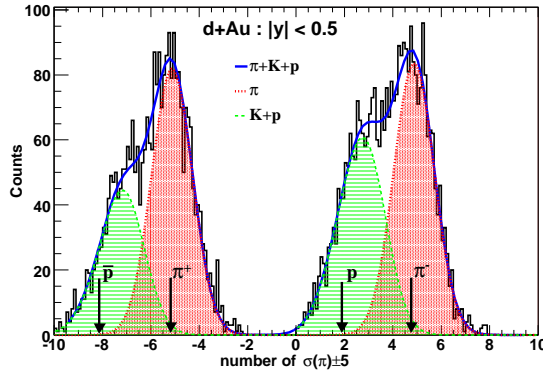


Fig. 1.  $dE/dx$  distribution normalized by pion  $dE/dx$  at  $4.5 < p_T < 5.0$  GeV/ $c$  and  $|\eta| < 0.5$ , and shifted by  $\pm 5$  for positively and negatively charged particles, respectively. The distributions are for minimum bias  $d+Au$  collisions. The pion, proton and anti-proton peak positions are indicated by arrows.

distribution about  $2.5\sigma$  away from the pion  $dE/dx$  peak. The integration limits were varied to check the stability of the results. Figure 1 shows a typical  $dE/dx$  distribution normalized by the pion  $dE/dx$  at  $4.5 < p_T < 5.0$  GeV/ $c$  and  $|\eta| < 0.5$ . The Gaussian distribution used to extract the pion yield and the pion, proton and anti-proton peak positions are also shown in the figure.

The kaon contamination is estimated via either of the equations given below. The raw count of the proton yield is

$$p = (Y - \beta(h - \pi))/(\alpha - \beta)$$

or

$$p = (Y - \beta K_S^0)/\alpha,$$

where  $\alpha$  and  $\beta$  are the proton and kaon efficiencies from the integration described above, derived from the  $dE/dx$  calibration, resolution and the Bichsel function [23]. In the first case the kaon contamination is estimated through the yields of the inclusive hadrons ( $h$ ) and pions, in case two from known yields from  $K_S^0$  measurements [23,24]. At high  $p_T$ , the yields of other stable particles (i.e., electrons and deuterons) are at least two orders of magnitude lower than those of pions, and are negligible in our studies. The two results are consistent where STAR  $K_S^0$  measurements are available. The  $p_T$  dependence of the reconstruction efficiency, background and the systematic uncertainties for pions, protons and anti-protons for low  $p_T$  in  $p+p$  and  $d+Au$  collisions are described in Ref. [22]. At high  $p_T$  ( $> 2.5$  GeV/ $c$ ), the efficiency is almost independent of  $p_T$  in both  $p+p$  and  $d+Au$  collisions. The tracking efficiency for pions, protons and anti-protons for  $p_T > 2.5$  GeV/ $c$  is  $\sim 88\%$  and  $92\%$  in  $p+p$  and  $d+Au$  collisions respectively. The efficiency is estimated by embedding Monte Carlo particles into the real data and then following the full reconstruction procedure. The background contamination to pion spectra for  $p_T > 2.5$  GeV/ $c$ , primarily from  $K_S^0$  weak decay is estimated from PYTHIA/HIJING



Table 1

Fit parameters for the Levy function (Eqn. 1) for hadrons in  $p+p$  and  $d+Au$  minimum bias collisions at  $\sqrt{s_{NN}} = 200$  GeV.

Type	$B$ (GeV/c) <sup>-2</sup>	$T$ (GeV)	$n$	$\chi^2/\text{ndf}$
$p+p$ ( $\pi^+$ )	$5.4 \pm 0.5$	$0.127 \pm 0.003$	$9.75 \pm 0.17$	9.60/20
$p+p$ ( $\pi^-$ )	$5.5 \pm 0.5$	$0.127 \pm 0.004$	$9.74 \pm 0.17$	8.90/20
$d+Au$ ( $\pi^+$ )	$13.2 \pm 1.2$	$0.151 \pm 0.003$	$10.10 \pm 0.17$	21.64/21
$d+Au$ ( $\pi^-$ )	$13.1 \pm 1.2$	$0.151 \pm 0.004$	$10.12 \pm 0.17$	13.10/21
$p+p$ ( $p$ )	$0.072 \pm 0.005$	$0.179 \pm 0.006$	$10.87 \pm 0.43$	24.84/17
$p+p$ ( $\bar{p}$ )	$0.061 \pm 0.005$	$0.173 \pm 0.006$	$10.49 \pm 0.40$	17.70/17
$d+Au$ ( $p$ )	$0.30 \pm 0.01$	$0.205 \pm 0.004$	$11.00 \pm 0.29$	21.19/20
$d+Au$ ( $\bar{p}$ )	$0.23 \pm 0.01$	$0.215 \pm 0.005$	$12.55 \pm 0.41$	26.40/20

simulations with full GEANT detector descriptions to be  $\sim 4\%$ . The charged pion spectra are corrected for efficiency and background effects. The inclusive proton and anti-proton spectra are presented with efficiency corrections and without hyperon feed-down corrections. The  $\Lambda/p$  ratio is estimated to be  $< 20\%$ . Additional corrections are applied for primary vertex reconstruction inefficiency as discussed in Ref. [15,16,22]. The momentum resolution is given as  $\Delta p_T/p_T = 0.01 + 0.005p_T/(\text{GeV}/c)$  and has  $< 4\%$  effect on the yields at the highest  $p_T$  value. The spectra are not corrected for momentum resolution effects, but they are included in the systematic errors.

The total systematic uncertainties associated with pion yields are estimated to be  $\lesssim 15\%$ . This systematic uncertainty is dominated by the uncertainty in modeling the detector response in the Monte Carlo simulations. Protons from hyperon ( $\Lambda$  and  $\Sigma$ ) decays away from the primary vertex can be reconstructed as primordial protons at a slightly higher  $p_T$  than their true value, but with worse momentum resolution. This results in an uncertainty of the inclusive proton yield of  $\sim 2\%$  at  $p_T = 3$  GeV/ $c$  and  $\sim 10\%$  at  $p_T = 10$  GeV/ $c$ . For proton and anti-proton yields at high  $p_T$  an additional systematic error arises from the uncertainties in the determination of the efficiencies,  $\alpha$  and  $\beta$ , under a specific  $dE/dx$  selection for integration. This is due to the uncertainties in the mean  $dE/dx$  positions for protons and kaons. The total systematic uncertainty in obtaining the proton and anti-proton yields for  $p_T > 2.5$  GeV/ $c$  increases with  $p_T$  from 12% to 22% (at  $p_T = 7$  GeV/ $c$ ) in both  $p+p$  and  $d+Au$  collisions. The errors shown in the figures are statistical, the systematic errors are plotted as shaded bands. In addition, there are overall normalization uncertainties from trigger and luminosity in  $p+p$  and  $d+Au$  collisions of 14% and 10%, respectively [15]. These errors are not shown.

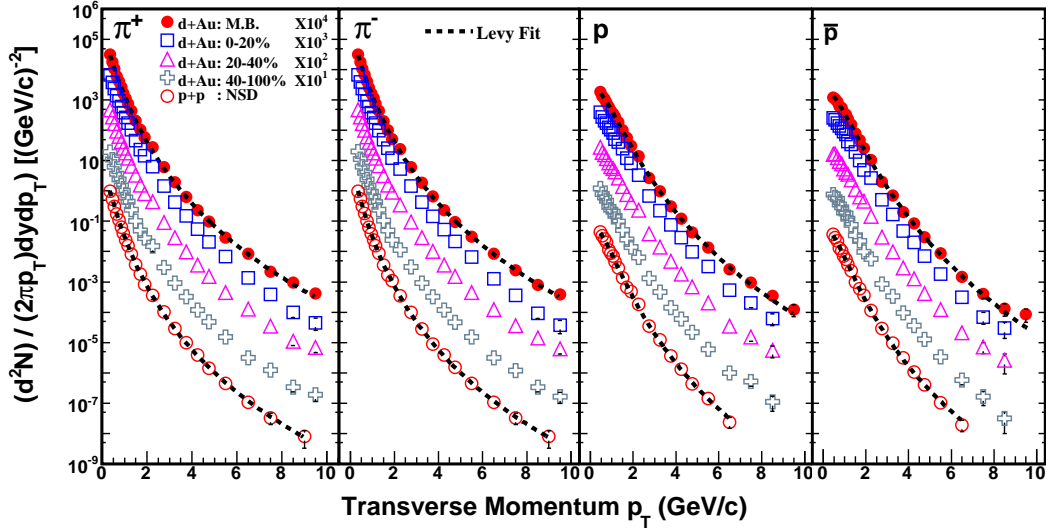


Fig. 2. Midrapidity ( $|y| < 0.5$ ) transverse momentum spectra for charged pions, proton and anti-proton in  $p+p$  and  $d+Au$  collisions for various event centrality classes. Minimum bias distributions are fit to Levy functions which are shown as dashed curves.

Figure 2 shows the invariant yields of charged pions, protons and anti-protons for the  $p_T$  range of  $0.3 < p_T < 10$  GeV/ $c$  in minimum bias  $p+p$  collisions and for various centrality classes in  $d+Au$  collisions. The yields span over eight orders of magnitude. The minimum bias distributions are fitted with a Levy distribution of the form

$$\frac{d^2N}{2\pi p_T dp_T dy} = \frac{B}{(1 + (m_T - m_0)/nT)^n} \quad (1)$$

where  $m_T = \sqrt{p_T^2 + m_0^2}$  and  $m_0$  is the mass of the hadron. The Levy distribution essentially takes a power-law form at higher  $p_T$  and has an exponential form at low  $p_T$ . The values of the fit parameters are given in Table 1. Both power-law and Levy distributions give reasonable fits to the data in  $p+p$  and pion production in  $d+Au$  collisions. For the proton and anti-proton spectra in  $d+Au$  collisions the Levy distribution gives a better fit compared to power-law.

### 3 Nuclear modification factor

The nuclear modification factor ( $R_{dAu}$ ) can be used to study the effects of cold nuclear matter on particle production. It is defined as a ratio of the invariant yields of the produced particles in  $d+Au$  collisions to those in  $p+p$  collisions

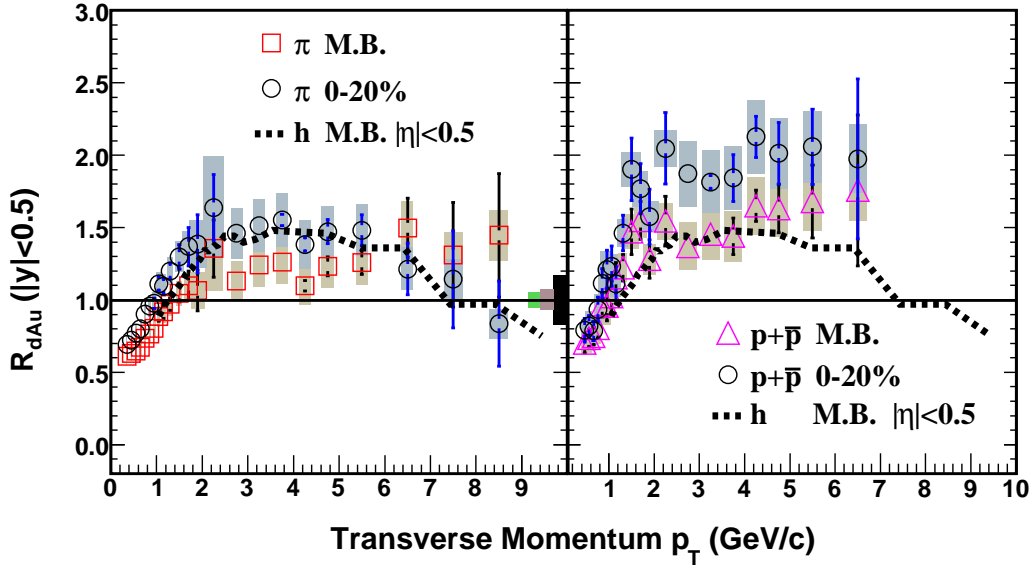


Fig. 3. Nuclear modification factor  $R_{dAu}$  for charged pions  $(\pi^+ + \pi^-)/2$  and  $p+\bar{p}$  at  $|y| < 0.5$  in minimum bias and 0-20% central  $d+Au$  collisions. For comparison results on inclusive charged hadrons (STAR) from Ref. [15] at  $|\eta| < 0.5$  are shown by dashed curves. The first two shaded bands around 1 correspond to the error due to uncertainties in estimating the number of binary collisions in minimum bias and 0-20% central  $d+Au$  collisions respectively. The last shaded band is the normalization uncertainty from trigger and luminosity in  $p+p$  and  $d+Au$  collisions.

scaled by the underlying number of nucleon-nucleon binary collisions.

$$R_{dAu}(p_T) = \frac{d^2 N_{dAu}/dydp_T}{\langle N_{bin} \rangle / \sigma_{pp}^{inel} d^2 \sigma_{pp}/dydp_T}, \quad (2)$$

where  $\langle N_{bin} \rangle$  is the average number of binary nucleon-nucleon (NN) collisions per event, and  $\langle N_{bin} \rangle / \sigma_{pp}^{inel}$  is the nuclear overlap function  $T_A(b)$  [15,16]. The  $\sigma_{pp}^{inel}$  is taken to be 42 mb.

The left panel of Fig. 3 shows  $R_{dAu}$  values for charged pions  $((\pi^+ + \pi^-)/2)$  in minimum bias and 0-20% central collisions at  $|y| < 0.5$ . The  $R_{dAu}$  for 0-20% central collisions are higher than  $R_{dAu}$  for minimum bias collisions. The result  $R_{dAu} > 1$  indicates a slight enhancement of high  $p_T$  charged pion yields in  $d+Au$  collisions compared to binary collision scaled charged pion yields in  $p+p$  collisions within the measured  $(y, p_T)$  range. The right panel of Fig. 3 shows the  $R_{dAu}$  of baryons ( $p+\bar{p}$ ) for the minimum bias collisions at  $|y| < 0.5$ . The  $R_{dAu}$  for  $p + \bar{p}$  is again greater than unity for  $p_T > 1.0$  GeV/c and is larger than that of the charged pions. The  $R_{dAu}$  of pions for  $2 < p_T < 5$  GeV/c is  $1.24 \pm 0.13$  and that for  $p+\bar{p}$  is  $1.49 \pm 0.17$  in minimum bias collisions.

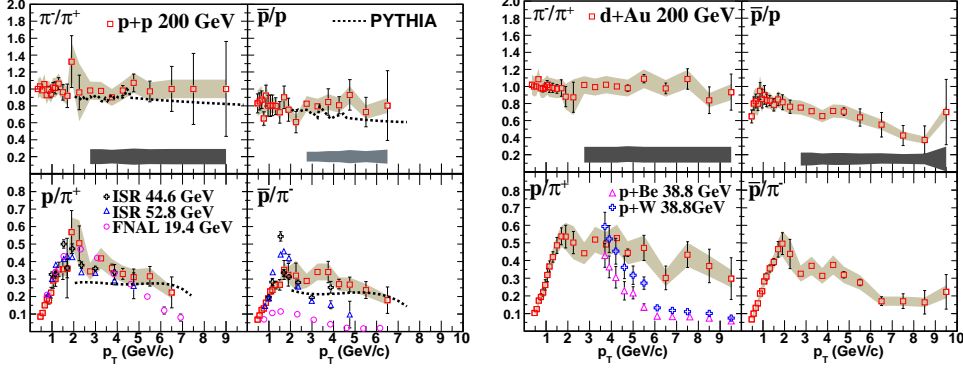


Fig. 4. Ratio of  $\pi^-/\pi^+$ ,  $\bar{p}/p$ ,  $p/\pi^+$ ,  $\bar{p}/\pi^-$  at midrapidity ( $|y| < 0.5$ ) as a function of  $p_T$  in  $p+p$  and  $d+Au$  minimum bias collisions. For comparison the results from lower energies at ISR [30] and FNAL [31] are also shown for  $p/\pi^+$  and  $\bar{p}/\pi^-$  ratios. The dotted curves in the results for  $p+p$  collisions are from PYTHIA. The shaded bands below the  $\pi^-/\pi^+$  and  $\bar{p}/p$  ratios are the point-to-point correlated errors in the yields associated with the ratio.

Recently, the inclusive charged hadron and  $\pi^0$   $R_{dAu}$  have been reasonably well-explained by various models. These models include different physics effects, such as only nuclear shadowing [25], transverse momentum broadening along with dynamical shadowing and energy loss in cold nuclear matter [26], a colour glass condensate approach [27], and hadronization through the recombination picture [28]. It may be possible that all these processes are contributing to the observed  $R_{dAu}$ , and the presented data on identified hadron  $R_{dAu}$  should be able to provide insight on relative contributions of the different processes and further constrain the models.

#### 4 Particle ratios

The particle ratios at midrapidity as a function of  $p_T$  for  $p+p$  and  $d+Au$  minimum bias collisions are shown in Fig. 4. The  $\pi^-/\pi^+$  ratio has a value  $\sim 1$  and is independent of  $p_T$  in both  $p+p$  and  $d+Au$  collisions. The  $\bar{p}/p$  ratio for  $p+p$  collisions is also independent of  $p_T$  within the range studied and has a value of  $0.81 \pm 0.1$  at  $2.5 < p_T < 6.5$  GeV/c. The shaded band below the data points for  $\pi^-/\pi^+$  and  $\bar{p}/p$  ratios in Fig. 4 represents the point-to-point correlated errors in the yields, arising mainly due to uncertainty in the determination of  $dE/dx$  peak positions for  $\pi^\pm$ ,  $p$  and  $\bar{p}$ , and momentum resolution effects. Calculations from PYTHIA(v6.319) predict somewhat more prominent  $p_T$  dependence [19]. However, in  $d+Au$  collisions we observe a clear decrease of  $\bar{p}/p$  for  $p_T > 6$  GeV/c. In quark fragmentation, the leading hadron is more likely to be a particle rather than an anti-particle, and there is no such preference from a gluon jet. A decrease in the antiparticle/particle ratio with  $p_T$  would then indicate a significant quark jets contribution to the baryon

production. It is, however, not clear whether the same effect exists in  $p+p$  collisions or whether the decrease of  $\bar{p}/p$  is due to additional nuclear effects in  $d+Au$  collisions. Future  $p+p$  data with high statistics should be able to answer this question. The  $\bar{p}/p$  ratio at lower FNAL energies (not shown in the figure) is smaller than the present data and shows a decreasing trend with  $p_T$  at high  $p_T$ .

At RHIC, the  $p/\pi^+$  and  $\bar{p}/\pi^-$  ratios increase with  $p_T$  up to 2 GeV/ $c$  and then start to decrease for higher  $p_T$  in both  $p+p$  and  $d+Au$  collisions. The  $\bar{p}/\pi^-$  ratio rapidly approaches a value of 0.2, which is in between the values in  $e^+e^-$  collisions for quark and gluon jets [7,29]. The  $p/\pi^+$  and  $\bar{p}/\pi^-$  ratios from PYTHIA is constant at high  $p_T$  in contrast to a decreasing trend observed in data. The  $p/\pi^+$  ratios in  $p+p$  collisions compare well with results from lower energy ISR and FNAL fixed target experiments [30,31], while  $\bar{p}/\pi^-$  ratios at high  $p_T$  has a strong energy dependence with larger values at higher beam energies. In  $d+Au$  collisions the  $p/\pi^+$  ratio at high  $p_T$  is lower for  $p+A$  collisions at FNAL energy than at RHIC.

## 5 Comparison to NLO pQCD and model calculations

In Fig. 5 we compare  $(\pi^+ + \pi^-)/2$  and  $(p+\bar{p})/2$  yields in minimum bias  $p+p$  and  $d+Au$  collisions at midrapidity for high  $p_T$  to those from NLO pQCD calculations and the EPOS model [32]. The NLO pQCD results are based on calculations performed with three sets of FFs, the *Kretzer* [33], the *Kniehl-Kramer-Potter (KKP)* [34] and the *Albino-Kniehl-Kramer (AKK)* set of functions [35]. The main difference between the Kretzer and KKP FFs is the way gluons fragment to pions. The gluon to pion FF is larger in the KKP set than the Kretzer set. The differences between the KKP and AKK FFs are as follows. The KKP FFs are obtained from  $e^+e^-$  collision data where the observed hadron is identified as a  $\pi^\pm$  or  $K^\pm$  or  $p(\bar{p})$  and the emitting parton is identified as either a gluon, light ( $u, d$ , and  $s$ ) quark,  $c$  quark or  $b$  quark; the AKK FFs use the recent data from the OPAL Collaboration [29] on light-flavor separated measurements of light charged hadron production in  $e^+e^-$  collisions [29], thereby allowing the extraction of the flavor-dependent FFs of light quarks. For NLO pQCD calculations in  $d+Au$  collisions, the parton distributions for the deuteron are obtained via the average of the distributions in protons and neutrons  $((p+n)/2)$  [36]. The parton distributions for gold nuclei are obtained by convoluting the free nucleon parton densities with simple weight functions that are meant to parametrize nuclear effects [37]. These are further constrained by comparing to deep inelastic scattering data off nuclei [37]. We observe that our charged pion data for  $p_T > 2$  GeV/ $c$  in  $p+p$  collisions are reasonably well explained by the NLO pQCD calculations using the KKP and AKK set of FFs (see Fig. 5). The factorization scale for

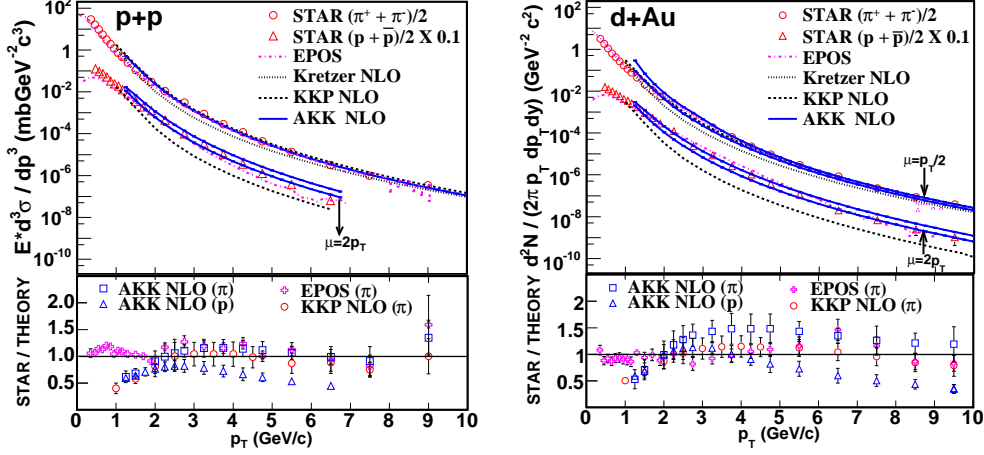


Fig. 5. Top panels: Midrapidity invariant yields for  $(\pi^+ + \pi^-)/2$  and  $(p+\bar{p})/2$  at high  $p_T$  for minimum bias  $p+p$  and  $d+Au$  collisions compared to results from NLO pQCD calculations using “Kretzer” [33], KKP [34] (PDF: CTEQ6.0) and AKK [35] (PDF: CTEQ6M) sets of fragmentation functions and results from the EPOS model [32]. Bottom panels: Ratio of STAR  $\pi$  and  $p + \bar{p}$  yields to the same from NLO pQCD calculations and the ratio of STAR  $\pi$  yields to those from EPOS model. All results from NLO pQCD calculations are with factorization scale  $\mu = p_T$ . Those with different scales are indicated in the figure.

all the NLO pQCD calculations shown is for  $\mu = p_T$  (unless specified). For  $d+Au$  collisions NLO pQCD calculations with KKP FFs are consistent with the data for  $p_T > 4$  GeV/ $c$  while those with AKK FFs overpredict the measured charged pion yields. For the calculations using AKK FFs we also show results for pion spectra with  $\mu = p_T/2$  in  $d+Au$  collisions, which are observed to be consistent with the data for  $p_T > 3$  GeV/ $c$ . The NLO pQCD calculations using the Kretzer set of FFs underestimate the charged pion data in both  $p+p$  and  $d+Au$  collisions. It may be mentioned that similar conclusions on KKP and Kretzer FF for  $\pi^0$  production ( $1 < p_T < 14$  GeV/ $c$ ) were obtained by the PHENIX Collaboration [38].

The proton+anti-proton yield in  $p+p$  and  $d+Au$  collisions is much higher than the results from NLO pQCD calculations using the KKP set of FFs and lower compared to calculations using AKK FFs for the factorization scale  $\mu = p_T$ . The proton+anti-proton yield in  $p+p$  collisions for  $p_T > 2$  GeV/ $c$ , however, is reasonably well explained by AKK set of FFs for  $\mu = 2p_T$  and for  $p_T > 5$  GeV/ $c$  in  $d+Au$  collisions. The relatively better agreement of NLO pQCD calculations with AKK FFs compared to those with KKP FFs for proton+anti-proton yields shows the importance of the flavor-separated measurements in  $e^+ + e^-$  collisions in determining the FFs for baryons. One may further improve the NLO pQCD calculations by an all-order resummation of large logarithmic corrections to the partonic cross-sections [39]. The NLO pQCD calculations for  $d+Au$  collisions are in reasonable agreement with the data at a higher  $p_T$  value compared to those for  $p+p$  collisions. This may be attributed to the

choice of nuclear PDFs and Cronin effect.

We also observe that the results from a phenomenological parton model (EPOS) [32] agree fairly well with our data for charged pions and proton+anti-proton in  $p+p$  and  $d+Au$  collisions. The EPOS model includes two important nuclear effects through elastic and inelastic parton ladder splitting. The elastic splitting is related to screening and saturation while the inelastic splitting is related to the hadronization process. The proton+anti-proton spectra from EPOS model is not corrected for the hyperon feed-down corrections.

## 6 Scaling of particle production

The invariant cross-sections of inclusive pion production in high energy  $p+p$  collisions have been found to follow the scaling laws [40] :

$$E \frac{d^3\sigma}{dp^3} = \frac{1}{p_T^n} f(x_T) \quad \text{or} \quad E \frac{d^3\sigma}{dp^3} = \frac{1}{\sqrt{s}^n} g(x_T) \quad (3)$$

where  $x_T = 2p_T/\sqrt{s}$  and  $f(x_T)$  and  $g(x_T)$  are some functions of  $x_T$ . Similar scaling has been observed in  $e^+e^-$  collisions, but without the  $\sqrt{s}^n$  or  $p_T^n$  factor [41]. The value of the power  $n$  ranges from 4 to 8 [42]. In the general scaling form  $\sim 1/p_T^n$ ,  $n$  depends on the quantum exchanged in the hard scattering. In parton models, it is related to the number of point-like constituents taking an active role in the interaction and its value reaches 8 in the case of a quark-meson scattering by exchanging a quark. With the inclusion of QCD, the scaling law follows as  $\sim 1/\sqrt{s}^n$ , where  $n$  becomes a function of  $x_T$  and  $\sqrt{s}$ . The value of  $n$  depends on the evolution of the structure function and FFs. A value of  $n=4$  is expected in more basic scattering processes (as in QED) [42,43].

Figure 6 shows the  $x_T$  scaling of pions, protons and anti-protons. The value of  $n$  obtained for the scaling with  $\sqrt{s}^n$  of the invariant cross-section is  $6.5 \pm 0.8$ . The data points deviate from the scaling behavior for  $p_T < 2$  GeV/ $c$  for pions and protons, which could be interpreted as a transition region from soft to hard processes in the particle production. The deviations start at a higher  $p_T$  for the anti-protons. The available data on pion and proton invariant cross-sections at various center-of-mass energies [4,30,31,38,40,44] for  $p_T > 2$  GeV/ $c$  are compiled and fit using a function  $\frac{1}{p_T^n} (1 - x_T)^m$ . The value of  $n$  ranges from 6.0 to 7.3 for  $\sqrt{s_{NN}}$  between 19 GeV and 540 GeV, while that for  $m$  ranges between 13 and 22. The average value of  $n$  for pions is  $6.8 \pm 0.5$  and that for protons and anti-protons is  $6.5 \pm 1.0$ . The variations in  $n$  and  $m$  values may lead to differences in details of scaling behaviour at different energies when the

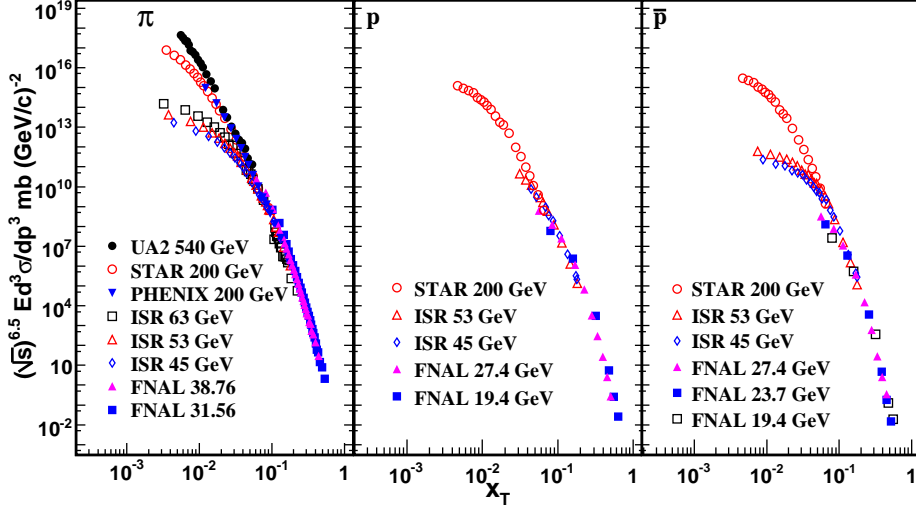


Fig. 6.  $x_T$  scaling of pions, protons and anti-protons. The data from other experiments are from the following references, FNAL : Refs [4,31], ISR : Ref. [30], PHENIX : Ref. [38], and UA2 [44]

cross-section is multiplied by  $1/p_T^n$  [45], a feature not observed in the scaling shown in Fig. 6 due to the data spanning several orders of magnitude. The spectra at  $p_T < 2$  GeV/c have been observed to follow a  $m_T$  scaling [24], consistent with possible transition between soft and hard processes at around  $p_T \simeq 2$  GeV/c. For  $m_T$  values greater than 2 GeV/c<sup>2</sup>, there is no scaling observed between charged pions and  $p+\bar{p}$ . This suggests that flow effects in  $p+p$  and  $d+Au$  collisions are negligible [8,9]. The presented data suggests that the transition region from soft to hard physics occurs around  $p_T \sim 2$  GeV/c in  $p+p$  collisions.

## 7 Summary

We have presented transverse momentum spectra for identified charged pions, protons and anti-protons from  $p+p$  and  $d+Au$  collisions at  $\sqrt{s_{NN}} = 200$  GeV. The transverse momentum spectra are measured around midrapidity ( $|y| < 0.5$ ) over the range of  $0.3 < p_T < 10$  GeV/c with particle identification from the ionization energy loss and its relativistic rise in the Time Projection Chamber, and the Time-of-Flight in STAR. The minimum bias identified particle spectra are well-described by the Levy distribution. The identified particle nuclear modification factor around midrapidity is found to be enhanced above unity for pions, while the effect on proton and anti-proton spectra is even larger at the intermediate  $p_T$  ( $2 < p_T < 5$  GeV/c). The  $\pi^-/\pi^+$ ,  $\bar{p}/p$ ,  $p/\pi^+$  and  $\bar{p}/\pi^-$  ratios have been studied at high  $p_T$ . The  $\pi^-/\pi^+$  and  $\bar{p}/p$  ratios in  $p+p$  collisions are independent of  $p_T$  in the measured range, a feature not predicted by PYTHIA calculations.  $p/\pi$  ratios peak at  $p_T \simeq 2$  GeV/c with a value of



$\sim 0.5$ , and then decrease to  $\sim 0.2$  at high  $p_T$  with the possible exception of the  $p/\pi^+$  ratio in  $d+\text{Au}$  collisions. The charged pions, and combined proton and anti-proton spectra in  $p+p$  and  $d+\text{Au}$  collisions have been compared to calculations from a phenomenological model (EPOS) and with the next-to-leading order perturbative QCD calculations with specific fragmentation schemes. The NLO pQCD calculations explain the high  $p_T$  data for charged pions reasonably well for  $p_T > 2 \text{ GeV}/c$  in  $p+p$  collisions and  $p_T > 4 \text{ GeV}/c$  for  $d+\text{Au}$  collisions. The high  $p_T$   $p+\bar{p}$  spectra are only explained by NLO pQCD calculations using the AKK set of FFs for the factorization scale of  $\mu = 2p_T$ . In general, baryon production has historically been difficult to describe by the pQCD and hadronization [43,46,47]. An improved description of experimental data in RHIC's  $p+p$  collisions by the AKK FFs, which comes from NLO pQCD fits to the  $e^+e^-$  data, is extremely interesting. These findings will provide a better foundation for constraining applications of jet quenching and quark recombination models to explain the phenomena in A+A collisions in this  $p_T$  range. We find that both the proton and pion spectra in  $p+p$  collisions follow  $x_T$ -scaling with a beam-energy dependent factor  $\sim \sqrt{s_{\text{NN}}}^{6.5}$  above  $p_T \sim 2 \text{ GeV}/c$ . Since the pion and proton spectra follow transverse mass scaling only in the  $1 < m_T < 2 \text{ GeV}/c^2$  region for both  $p+p$  and  $d+\text{Au}$  collisions we conclude that the transition region from soft to hard process domination occurs at  $p_T \sim 2 \text{ GeV}/c$  in these collision systems.

We would like to thank Werner Vogelsang, Stefan Kretzer and Simon Albino for providing us the NLO pQCD results, Klaus Werner for the EPOS results and J. Raufeisen for useful discussions. We thank the RHIC Operations Group and RCF at BNL, and the NERSC Center at LBNL for their support. This work was supported in part by the HENP Divisions of the Office of Science of the U.S. DOE; the U.S. NSF; the BMBF of Germany; IN2P3, RA, RPL, and EMN of France; EPSRC of the United Kingdom; FAPESP of Brazil; the Russian Ministry of Science and Technology; the Ministry of Education and the NNSFC of China; IRP and GA of the Czech Republic, FOM of the Netherlands, DAE, DST, and CSIR of the Government of India; Swiss NSF; the Polish State Committee for Scientific Research; STAA of Slovakia, and the Korea Sci. & Eng. Foundation.

## References

- [1] J. C. Collins and D. E. Soper, Ann. Rev. Nucl. Part. Sci. 37 (1987) 383; J. C. Collins, D. E. Soper and G. Sterman in Perturbative Quantum Chromodynamics (World Scientific, 1989) edited by A. H. Muller and Adv. Ser. Direct. High Energy Phys. 5 (1988) 1; G. Sterman et al., Rev. Mod. Phys. 67 (1995) 157.
- [2] R. D. Field and R. P. Feynman, Nucl. Phys. B 136 (1978) 1; J. F. Owens, Rev.

Mod. Phys. 59 (1987) 465.

- [3] D. E. Soper, Nucl. Phys. B (Proc. Suppl.) 53 (1997) 69; A. D. Martin, W. J. Stirling and R.G. Roberts, Phys. Lett. B 354 (1995) 155; M. Gluck, E. Reya and A. Vogt, Z. Phys. C 67 (1995) 433; H. L. Lai et al., Phys. Rev. D 51 (1995) 4763.
- [4] D. Antreasyan et al., Phys. Rev. D 19 (1979) 764.
- [5] L. McLerran and R. Venugopalan, Phys. Rev. D 49 (1994) 2233; Phys. Rev. D 50 (1994) 2225.
- [6] P. B. Straub et al., Phys. Rev. D 45 (1992) 3030.
- [7] DELPHI Collaboration, P. Abreu et al., Eur. Phys. J. C 5 (1998) 585; Eur. Phys. J. C 17 (2000) 207.
- [8] BRAHMS Collaboration, I. Arsene et al., Nucl. Phys. A 757 (2005) 1; PHOBOS Collaboration, B.B. Back et al., Nucl. Phys. A 757 (2005) 28; STAR Collaboration, J. Adams et al., Nucl. Phys. A 757 (2005) 102; PHENIX Collaboration, K. Adcox et al., Nucl. Phys. A 757 (2005) 184.
- [9] D. Teaney, J. Lauret, E.V. Shuryak, arXiv:nucl-th/0110037.
- [10] V. Greco, C.M. Ko and P. Levai, Phys. Rev. Lett. 90 (2003) 202302; R. J. Fries, B. Muller, C. Nonaka and S. A. Bass, Phys. Rev. Lett. 90 (2003) 202303.
- [11] STAR Collaboration, C. Adler et al., Phys. Rev. Lett. 90 (2003) 082302; PHENIX Collaboration, S.S. Adler et al., Phys. Rev. Lett. 91 (2003) 072301.
- [12] STAR Collaboration, J. Adams et al., Phys. Rev. Lett. 92 (2004) 052302.
- [13] X.-N. Wang and M. Gyulassy, Phys. Rev. Lett. 68 (1992) 1480.
- [14] K. H. Ackerman et al., Nucl. Instrum. Meth. A 499 (2003) 624.
- [15] STAR Collaboration, J. Adams et. al, Phys. Rev. Lett. 91 (2003) 072304.
- [16] STAR Collaboration, J. Adams et. al, Phys. Rev. Lett. 92 (2004) 112301.
- [17] S. N. White, arXiv:nucl-ex/0507023.
- [18] STAR Collaboration, J. Adams et al., Phys. Rev. Lett. 91 (2003) 172302.
- [19] T. Sjostrand et al., Comput. Phys. Commun. 135 (2001) 238.
- [20] G. Corcella et al., JHEP 0101 (2001) 010.
- [21] A. Drees and Z. Xu, Proceedings of the Particle Accelerator Conference 2001, Chicago, Il, p. 3120.
- [22] STAR Collaboration, J. Adams et. al, Phys. Lett. B 616 (2005) 8.
- [23] M. Shao et al., arXiv:nucl-ex/0505026.

- [24] M. Heinz (for STAR Collaboration), J. Phys. G 31 (2005) S1011; arXiv:nucl-ex/0505025.
- [25] R. Vogt, Phys. Rev. C 70 (2004) 064902.
- [26] J. Qiu and I. Vitev, arXiv:hep-ph/0405068.
- [27] D. Kharzeev, Y. Kovchegov and K. Tuchin, Phys. Lett. B 599 (2004) 23.
- [28] R. C. Hwa and C.B. Yang, Phys. Rev. Lett. 93 (2004) 082302.
- [29] OPAL Collaboration, G. Abbiendi et al., Eur. Phys. J. C 16 (2000) 407.
- [30] British-Scandinavian Collaboration, B. Alper et al., Nucl. Phys. B 100 (1975) 237.
- [31] E706 Collaboration, L. Apanasevich et al., Phys. Rev. D 68 (2003) 052001.
- [32] K. Werner, F. Liu and T. Pierog, arXiv:hep-ph/0506232.
- [33] S. Kretzer, Phys. Rev. D 62 (2000) 054001.
- [34] B. A. Kniehl, G. Kramer and B. Potter, Nucl. Phys. B 597 (2001) 337.
- [35] S. Albino, B. A. Kniehl and G. Kramer, Nucl. Phys. B 725 (2005) 181.
- [36] B. A. Kniehl and L. Zwirner, Nucl. Phys. B 637 (2002) 311.
- [37] L. Frankfurt, V. Guzey and M. Strikman, Phys. Rev. D 71 (2005) 054001; D. de Florian and R. Sassot, Phys. Rev. D 69 (2004) 074028.
- [38] PHENIX Collaboration, S.S. Adler et al, Phys. Rev. Lett. 91 (2003) 241803.
- [39] D. de Florian and W. Vogelsang, Phys. Rev. D 71 (2005) 114004.
- [40] A. G. Clark et al., Phys. Lett. B 74 (1978) 267; CCOR Collaboration, A. L. S. Angelis et al., Phys. Lett. B 79 (1978) 505; PHENIX Collaboration, S.S. Adler et al., Phys. Rev. C 69 (2004) 034910.
- [41] TPC Collaboration, H. Aihara et al., Phys. Rev. Lett. 61 (1988) 1263; ALEPH Collaboration, D. Buskulic et al., Z. Phys. C 66 (1995) 355; ARGUS Collaboration, H. Albrecht et al., Z. Phys. C 44 (1989) 547.
- [42] S. M. Berman, J. D. Bjorken and J. B. Kogut, Phys. Rev. D 4 (1971) 3388; R. Blankenbecler, S. J. Brodsky and J.F. Gunion, Phys. Lett. B 42 (1972) 461; J.F. Owens, E. Reya, M. Gluck, Phys. Rev. D 18 (1978) 1501.
- [43] S. Ekelin and S. Fredriksson, Phys. Lett. B 149 (1984) 509.
- [44] UA2 Collaboration, M. Banner et al., Phys. Lett. B 115 (1982) 59.
- [45] S. J. Brodsky, H. J. Pirner and J. Raufeisen, arXiv:hep-ph/0510315.
- [46] X. Zhang, G. Fai, and P. Levai, Phys. Rev. Lett. 89 (2002) 272301.
- [47] B. Andersson, G. Gustafson, T. Sjostrand, Phys. Scripta 32 (1985) 574; Nucl. Phys. B 197 (1982) 45.